



Optimized Copyright Protection of Scale-Adaptive Saliency-Driven ROI of Medical Records with MSER-Based authentication

Divyanshu Awasthi^{1,*} and Vinay Kumar Srivastava²

¹ Department of Electronics and Communication Engineering, GLA University, Mathura 281406, India

² Department of Electronics and Communication Engineering, Motilal Nehru National Institute of Technology Allahabad, Prayagraj, Uttar Pradesh 211004, India

Abstract

The medical information is always vulnerable to security violations. After the COVID-19 pandemic, the volume of medical information has exponentially increased and the major information is in the form of images. So, the security of this image information is crucial during the transfer using modern information and communication technologies from one place to another. Image watermarking is one of the methods to protect the copyright and integrity of medical records. The medical images consist of some area that has vital information regarding the disease and this area will be considered as the region of interest (ROI). Therefore, the protection of the copyright of this vital area is crucial for the effective diagnosis. The proposed technique utilizes a scale-adaptive anatomical saliency and a statistical information-guided ROI detection technique. The redundant wavelet transform (RDWT) and diagonalized Hessenberg

decomposition (Diag-HD), along with the discrete cosine transform (DCT), are used for watermark embedding and extraction procedures. To get the optimized scaling weight, nature-inspired Salp Swarm Optimization (SSO) is used. Maximally stable extremal regions (MSER) are used for feature-based authentication. The simulation results analysis demonstrates the effectiveness in terms of visual similarity and robustness of the proposed technique. The experimental results obtained also highlight the superiority of the proposed technique over other existing methods in terms of imperceptibility and robustness.

Keywords: region of interest, watermarking, optimization, authentication.

1 Introduction

In the current era of multimedia advancement, it is challenging to protect the integrity of multimedia content, including text, photos, videos, and audio [1]. By editing, amending, and changing the contents, an unauthorized user can change the essence of information. Images are the most important information carrier for healthcare communication in this digital age. The high risk of alteration and



Submitted: 10 December 2025

Accepted: 06 January 2026

Published: 10 February 2026

Vol. 2, No. 1, 2026.

10.62762/TISC.2025.898154

*Corresponding authors:

Divyanshu Awasthi
divyanshu.awasthi@gla.ac.in

Citation

Awasthi, D., & Srivastava, V. K. (2026). Optimized Copyright Protection of Scale-Adaptive Saliency-Driven ROI of Medical Records with MSER-Based authentication. *ICCK Transactions on Information Security and Cryptography*, 2(1), 43–54.

© 2026 ICCK (Institute of Central Computation and Knowledge)

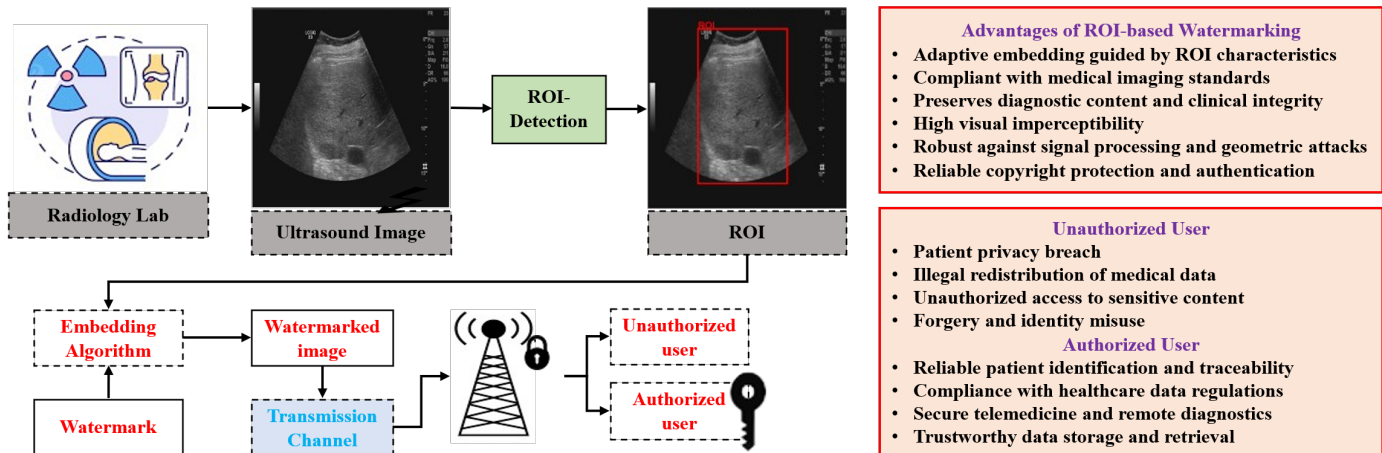


Figure 1. Overall framework of the proposed ROI-based watermarking scheme for medical image copyright protection.

tampering of image data without any owners consent is always there due to its vital necessity in medical domain [2]. So, the digital image watermarking can be used to protect the integrity of these critical medical images [3]. During the watermarking process, a watermark image is embedded in the host having high robustness and visual similarity for copyright protection during transmission. At the transmission end, the hidden watermark is then extracted using shared keys to check any violations. Applications for this method include remote sensing, healthcare, drone image protection, and the military. The medical image contain the vital ROI section, which contains the crucial information suitable for effective diagnosis. So, this vital information needs to be protected against any type of alterations when transmitted from patient to healthcare worker using modern internet technologies. The overall ROI-based watermarking framework is illustrated in Figure 1.

The following are the contributions of the proposed scheme:

- **ROI and RONI detection:**

The proposed method utilizes structural saliency and statistical abnormality characteristics in tandem to identify the ROI and RONI of medical ultrasound images. The main goal of this approach is to precisely locate diagnostically important areas without depending on training data or previous annotations, guaranteeing resilience, interpretability, and generalizability across various imaging modalities.

- **Efficient hybrid transform combination:**

The proposed scheme utilizes an effective combination of DCT, RDWT, and Diag-HD for the watermarking process. The complementary

advantages of frequency, multiresolution, and matrix-based representations are made possible by this combination. Dia-HD improves numerical stability and embedding dependability, RDWT adds shift invariance and spatial resilience, and DCT guarantees energy compaction and compression robustness. Watermark imperceptibility, resilience to geometric and signal processing attacks, and extraction accuracy are all enhanced by this synergistic combination.

- **Optimized Scaling weight:**

To obtain the optimum scaling weight, the SSO technique [4] is used in the proposed work. With less parameter tuning, its leader-follower system offers steady and effective search [5]. By optimizing embedding parameters, it successfully strikes a compromise between robustness and imperceptibility in watermarking, while maintaining diagnostic quality in medical imaging with minimal computational overhead.

- **MSER-based feature authentication:**

The MSER technique is employed for feature authentication due to its ability to detect highly stable and repeatable regions under intensity variations [6]. MSER features exhibit strong invariance to illumination changes, compression, and moderate geometric distortions, making them reliable for authentication and feature verification of medical records.

The remainder of the work is organized as follows: a detailed analysis of existing state-of-the-art techniques is presented in Section 2. Section 3 elaborates the proposed ROI-RONI detection algorithm, watermarking scheme, and optimization technique. Simulation results and their discussion are mentioned

in Section 4. Section 5 is related to the comparative analysis, while the conclusion and future scope are elaborated in Section 6.

2 Related Work

This section elaborates about the existing integrity protection techniques. A method for integrity protection of the ROI of the received medical image is proposed by Eswaraiah et al. [7]. This work uses a novel fragile block-based medical picture watermarking technique to prevent embedding distortion inside the ROI, confirm ROI integrity, precisely identify tampered blocks inside the ROI, and recover the original ROI with no loss. This technique divides the medical image into three groups of pixels: border pixels, ROI pixels, and RONI pixels [7]. Ravichandran et al. [8] examined the three major issues related to the e-healthcare that are as follows: (1) verification guarantee to the medical records; (2) data mismatch prevention for efficient and correct diagnosis; (3) preventing inadvertent or deliberate modification of medical images. The wavelet transform in integer (IWT) domain is by this scheme for watermarking. Das et al. [9] proposed a fragile and blind, ROI-based watermarking which is having lossless nature. This scheme offers a solution tool for a variety of medical data dissemination and management problems, including captioning, content authentication, secure archiving, controlled access retrieval, and security. In [10], IWT is used to protect the copyright of medical images during transmission. This approach provides better robustness to the RONI (Region of Non-Interest) data, accurately detects tampered blocks within ROI, and restores the original ROI. Keshavarzian et al. [11] proposed a blind and robust ROI watermarking using Arnold scrambling. ROI of the image is treated as the watermark. Bhalerao et al. [12] proposed a method with ROI tamper detection and recovery capabilities. The prediction-error expansion technique has been used to embed authentication data in the ROI region. The MSER feature extraction approach is used in [13] to separate medical images into ROI and RONI. Using the patient's Aadhar card and fingerprint pictures, a hybrid watermark image is created. Then this watermark is used to safeguard the ROI of the medical records [13].

A blind reversible watermarking technique is given by Qasim et al. [14] to identify both deliberate and inadvertent alterations in brain magnetic resonance images. The ROI and RONI are the two sections

into which the scheme divides images. Reversible watermarking based on the Difference Expansion approach is used to encode watermark data into the ROI [14]. The technique is protected from ownership attacks in [15] by using principal components-based insertion. In contrast, Lempel-Ziv-Welch-based fragile watermarking is employed to conceal the ROI of compressed images in order to counteract deliberate tampering attempts. The multiresolution domain approach is successfully applied with RDWT and multiresolution singular value decomposition (MSVD) in [16]. Frequency components are extracted using DCT. The optimal weighing factor is obtained by optimization using an adaptive neuro-fuzzy inference system (ANFIS). A method for watermarking that makes use of the essential components of the MSER and ANFIS was introduced by Awasthi et al. [17]. The ROI is calculated with the help of the MSER method and then encoded with a hybrid watermark. A hybrid watermark is created using two medical photos to improve the privacy of medical data. RDWT and DCT were combined for watermarking by Dwivedi et al. [18]. A logo and text image are embedded using QR decomposition and Randomized Singular Value Decomposition (RSVD) algorithms. To improve security, the watermarks are encrypted prior to embedding via chaotic logistic mapping. White Shark Optimization is used to determine the strength factor's ideal value. To balance imperceptibility and robustness, the embedding procedure in [19] incorporates lifting wavelet transform, Hessenberg decomposition, and singular value decomposition.

A blind medical watermarking method combining adaptive quantization modulation, Ant colony optimization, Ridgelet transform, and QR decomposition is mentioned in [20]. The Ridgelet transform identifies linear features that are crucial for diagnosis, while QR decomposition stabilizes coefficients against noise and compression. This method will be made even more resilient against geometric attacks. A watermarking method that uses a second-level discrete wavelet transform to first break down medical data is presented in [21]. Both the watermark and the frequency sub-band of medical images are subjected to further singular value decomposition. In order to maximize the strength factor of the watermarking method using a fitness function, a number of nature-inspired optimization techniques have been taken into consideration and examined here. The resilience against different attacks can be further enhanced. A watermarking method

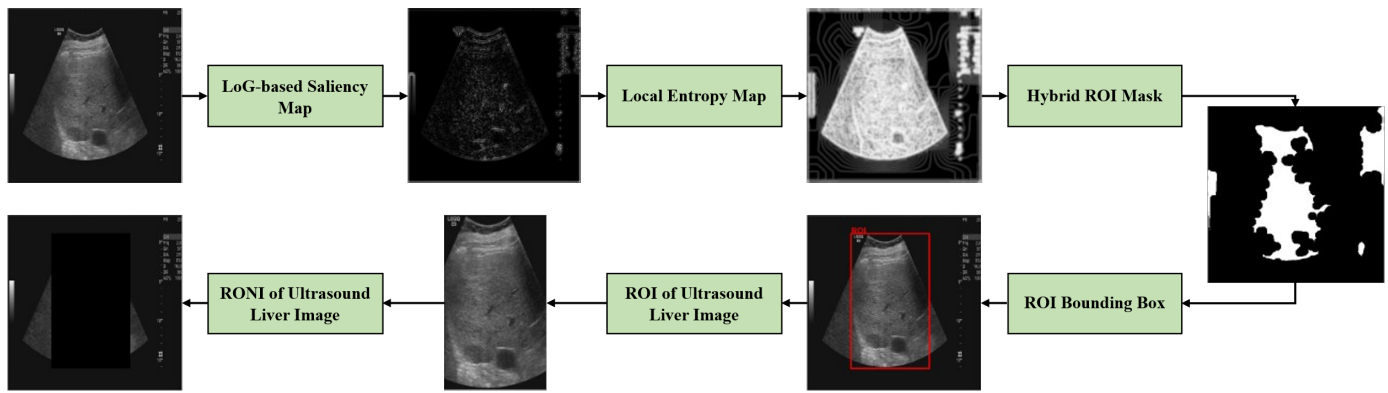


Figure 2. ROI-based watermarking framework.

that uses a second-level discrete wavelet transform to first break down medical data is presented in [22]. Both the watermark and the frequency sub-band of medical images are subjected to further singular value decomposition. In order to maximize the strength factor of the watermarking method using fitness function, a number of nature-inspired optimization techniques have been taken into consideration and examined here, including artificial bee colonies, bacterial foraging optimization, firefly algorithms, genetic algorithms, and particle swarm optimization [22]. The watermarked picture in [23] is encrypted using Arnold-cat map encryption, and the watermarked image and the cover image's FAST features are compared for authentication. The

suggested approach makes use of hybrid optimization approaches based on harmony search optimization and gray wolf optimization. The above-mentioned existing techniques have many advantages, but also have various drawbacks that motivate us to propose an efficient ROI-based optimized watermarking scheme.

3 Proposed Technique

The proposed technique protects the integrity of the ROI of medical data. RDWT, diagonalized Hessenberg decomposition and DCT are used for watermarking. Finally, MSER-based feature authentication is also carried out.

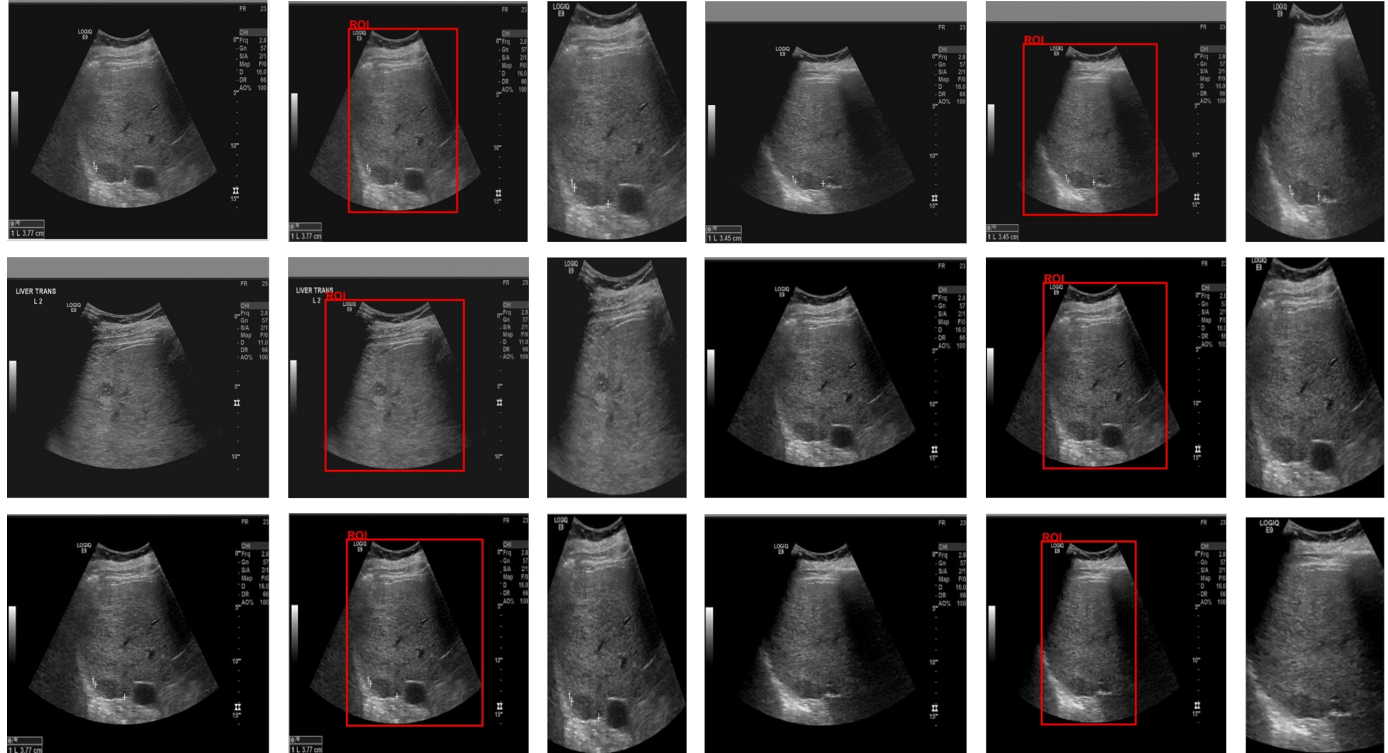


Figure 3. Various host images with bounding boxes and corresponding ROI.

3.1 ROI detection technique

The proposed technique uses a scale-adaptive saliency and statistical information-guided ROI detection scheme. Algorithm 1 presents a hybrid approach for automatic ROI detection by combining anatomical saliency and statistical texture information derived from the image. Contrast enhancement using adaptive histogram equalization and edge-preserving denoising is first applied to improve local intensity discrimination while maintaining anatomical boundaries. Structural saliency is extracted using a scale-adaptive LoG operator that emphasizes high-curvature and boundary-rich regions, while local entropy identifies statistically irregular and texturally complex areas. These complementary cues are fused to localize the most informative anatomical region, which is further refined using morphological operations and connected component analysis to ensure spatial coherence. The approach avoids the need for training data, reduces false-positive detections, and remains robust to noise and contrast variations across imaging conditions. Figure 2 illustrates the ROI and RONI detection procedure, while Figure 3 shows the various host images, along with the corresponding ROI and RONI.

3.2 Watermarking Procedure

The proposed system utilizes the efficient fusion of DCT [13], RDWT [24], and Diag-HD [25] for the watermarking process. The SSO is employed to obtain the effective scaling factor. Algorithm 2 and 3 shows the detailed description of the proposed watermarking Scheme.

3.3 Salp Swarm Optimization Procedure

Salps have transparent barrel-structured bodies and belong to the Salpidae family. Their tissues resemble those of jellyfish. Additionally, they move very similarly to jellyfish, which propel themselves ahead by pumping water through their bodies [24]. To update the position of the leader, the following equation is used [24]:

$$Z_i^1 = \begin{cases} P_i + r_1((u_i - l_i)r_2 + l_i), & r_3 \geq 0 \\ P_i - r_1((u_i - l_i)r_2 + l_i), & r_3 < 0 \end{cases} \quad (1)$$

In Eq. (1):

- Z_i^1 is the position of leader.
- P_i is the food source position (ℓ^{th} dimension).
- u_i is the upper limit (bound).

Algorithm 1: ROI and RONI Detection Technique

```

Input: Host image  $I^h$ 
Output: ROI, RONI
 $I^{enh} \leftarrow \text{adaphisteq}(I^h, \text{'ClipLimit'}, 0.01,$ 
     $\text{'NumTiles'}, [8, 8])$  ;
 $I^{fit} \leftarrow \text{imgaussfilt}(\text{wiener2}(I^{enh}, [5, 5]), 0.6)$  ;
 $\sigma \leftarrow 2.0$  ;
 $LoG \leftarrow \text{imfilter}(I^{fit},$ 
     $\text{fspecial('log', ceil(6\sigma), \sigma), 'replicate'})$  ;
 $SaliencyMask \leftarrow \text{imbinarize}(\text{mat2gray}(|LoG|),$ 
     $\text{graythresh}(\cdot))$  ;
 $EntropyMap \leftarrow$ 
     $\text{mat2gray}(\text{entropyfilt}(I^{fit}, \text{true}(9)))$  ;
 $EntropyMask \leftarrow \text{imbinarize}(EntropyMap,$ 
     $\text{graythresh}(EntropyMap))$  ;
 $HybridMask \leftarrow SaliencyMask \& EntropyMask$  ;

 $HybridMask \leftarrow \text{bwareaopen}($ 

     $\text{imfill}(\text{imclose}(HybridMask, \text{strel('disk', 12)}),$ 
     $\text{'holes'}), 500)$  ;
 $CC \leftarrow \text{bwconncomp}(HybridMask)$  ;
 $[], idx] \leftarrow \text{max}(\text{cellfun}(@\text{numel},$ 
     $CC.\text{PixelIdxList}))$  ;
 $FinalMask \leftarrow \text{false}(\text{size}(HybridMask))$  ;
 $FinalMask(CC.\text{PixelIdxList}\{idx\}) \leftarrow \text{true}$  ;
 $bbox \leftarrow \text{round}(\text{regionprops}(FinalMask,$ 
     $\text{'BoundingBox'}).BoundingBox)$  ;
 $X \leftarrow bbox(1); Y \leftarrow bbox(2)$  ;
 $Width \leftarrow bbox(3); Height \leftarrow bbox(4)$  ;
 $ROI \leftarrow I^h(Y : Y + Height, X : X + Width)$  ;
 $b \leftarrow \text{zeros}(512)$  ;
 $b(Y : Y + Height, X : X + Width) \leftarrow ROI$  ;
 $RONI \leftarrow I^h - b$  ;
return ROI, RONI ;

```

- l_i is the lower limit (bound).
- r_1, r_2, r_3 are the random numbers.

In Eq. (1), r_1 balances the exploration and exploitation as mentioned in Eq. (2):

$$r_1 = 2e^{-(\frac{4t}{T})^2} \quad (2)$$

where t is the current iteration and T is the maximum number of iterations.

Eq. (3) is used to update the followers' positions as shown below [20]:



Figure 4. Extracted watermark images.

$$Z_i^j = \frac{1}{2}v^{\text{final}}W^2 + v^oW \quad (3)$$

where $j \geq 1$; Z_i^j is the position of follower in ℓ^{th} dimension; v^o : initial speed.

To remove the discrepancy, the initial speed is taken as zero and time as 1. Eq. (3) will be expressed as mentioned in Eq. (4):

$$Z_i^j = \frac{1}{2}(Z_i^j + Z_i^{j-1}) \quad (4)$$

Eq. (5) is optimized using the SSO technique to get the optimum scaling weight:

$$\text{fitness} = \left(\text{SSIM} + \frac{\text{PSNR}}{100} \right) + \left(\frac{1}{\text{NCC} + \text{BER} + \text{KLD}} \right) \frac{1}{\mu} \quad (5)$$

In Eq. (5), PSNR is the peak signal to noise ratio [1], SSIM is the structure similarity index measure [1], KLD is the Kullback-Leibler distance [13], JSD is the Jensen-Shannon divergence [13], NCC is the normalized correlation coefficient [1], and BER is the bit error rate. μ is the number of parameters used.

The following are the advantages of the SSO technique over other metaheuristic schemes:

- An effective exploration-exploitation balance that prevents early trapping in local optima and allows

Algorithm 2: Watermarking Scheme: Embedding Procedure

```

Input: Host image ( $I^h$ ); Scaling weight ( $\omega$ )
Output: Watermarked image (marked)
 $I^h = \text{imread('Ultrasound liver image')};$ 
 $[ROI, RONI] = ROI\_RONI(I^h);$ 
 $M1 = \text{dct2}(ROI);$ 
 $M = M1(1 : 128, 1 : 128);$ 
 $[LLI, LHI, HLH, HH] = \text{RDWT}(M);$ 
 $[Q^1, R^1] = \text{hess}(LLI);$ 
 $d^1 = \text{diag}(R^1);$ 
 $D^1 = \text{diag}(d^1);$ 
 $s^1 = R^1 - D^1;$ 
 $I^w = \text{imread('Aadhar\_Card')};$ 
 $[LLW, LHW, HLW, HHW] = \text{RDWT}(I^w);$ 
 $[Q^w, R^w] = \text{hess}(HHW);$ 
 $d^w = \text{diag}(R^w);$ 
 $D^w = \text{diag}(d^w);$ 
 $s^w = R^w - D^w;$ 
 $SS^2 = D^1 + \omega \times D^w;$ 
 $S^2 = s^1 + SS^2;$ 
 $||1|| = Q^1 \times S^2 \times Q^1;$ 
 $L_1 = \text{iRDWT}(|1|, LHI, HLH, HH);$ 
 $M1(1 : 128, 1 : 128) = L_1;$ 
 $\text{inv} = \text{idct2}(M1);$ 
 $a^1 = \text{inv};$ 
 $b^1 = \text{zeros}(512);$ 
 $b^1(Y : Y + \text{Height}, X : X + \text{Width}) = a^1;$ 
 $\text{marked} = b^1 + RONI;$ 
return marked;

```

Algorithm 3: Watermarking Scheme: Extraction Procedure

```

Input: marked; Scaling weight ( $\omega$ )
Output: Extracted watermark ( $I^{ex}$ )
 $w_{ex} = \text{marked}(Y : Y + \text{Height}, X : X + \text{Width});$ 
 $\text{main1} = \text{dct2}(w_{ex});$ 
 $Mw = \text{main1}(1 : 128, 1 : 128);$ 
 $[LL1_{ex}, LH1_{ex}, HL1_{ex}, HH1_{ex}] = \text{RDWT}(Mw);$ 
 $[QW1, RW1] = \text{hess}(LL1_{ex});$ 
 $d1w = \text{diag}(RW1);$ 
 $D1w = \text{diag}(d1w);$ 
 $sw2 = (D1w - D^1)/\omega;$ 
 $Sw2 = sw2 + s^w;$ 
 $hh1ex = Q^w \times Sw2 \times Q^w;$ 
 $I^{ex} = \text{iRDWT}(LLW, LHW, HLW, hh1ex);$ 
return  $I^{ex};$ 

```

for quick convergence.

- The algorithm's straightforward structure and

reduced number of control parameters make it simple to implement and adjust.

- Excellent optimization performance for complicated and multimodal problems due to its strong ability to escape local minima.
- Compared to many other metaheuristic techniques, it has a low computational complexity, which results in a shorter execution time.

4 Simulation results and discussion

The proposed scheme uses the ultrasound image of the liver (UI) [27] of size 512×512 as the host. The Aadhar card identity of the patient, having a size of 128×128 , is taken as the watermark image. To analyze the imperceptibility, PSNR [1], SSIM [1], KLD [13], and JSD [13] are evaluated. Table 1 shows the values of performance parameters, in which the highest PSNR value attained is 65.5920 dB, and the SSIM is 1.0000. The optimum values of KLD and JSD are 0.021 and 0.0012, respectively. To analyze the resilience against various attacks, NCC [1] and BER [1] are calculated. The optimized NCC value attained is 1.0000 and the BER is 0.0029, as mentioned in Table 1. Table 2 shows the robustness of the proposed method in terms of NCC values against various attacks, while Table 3 demonstrates the resilience against combinational hybrid attacks. It clearly shows that the proposed method is highly robust and imperceptible. Figure 4 shows the extracted watermark images against various attacks.

Table 1. Performance parameter values.

Ultrasound image	PSNR	SSIM	NCC	JSD	KLD	BER
UI1	64.4573	1.0000	1.0000	0.0031	0.032	0.0084
UI2	63.5830	1.0000	1.0000	0.0012	0.041	0.0029
UI 3	63.5593	1.0000	1.0000	0.0035	0.043	0.0048
UI 4	64.3059	1.0000	1.0000	0.0061	0.033	0.0038
UI 5	64.5931	1.0000	1.0000	0.0053	0.037	0.0029
UI 6	65.1942	1.0000	1.0000	0.0045	0.021	0.0067
UI 7	65.1049	1.0000	1.0000	0.0024	0.020	0.0060
UI 8	65.5920	1.0000	1.0000	0.0042	0.024	0.0063
UI 9	65.4720	1.0000	1.0000	0.0027	0.023	0.0096
UI 10	64.4104	1.0000	1.0000	0.0064	0.022	0.0034
Average of 50 UI host images	64.0482	1.0000	1.0000	0.0021	0.024	0.0045

In the proposed technique, the average time required for ROI detection is 0.2978 seconds, while watermark embedding and extraction take 0.1709 seconds and 0.0722 seconds, respectively, demonstrating the computational efficiency of the method.

A traditional region-based feature identification method, the MSER technique finds related elements

Table 2. NCC values against attacks.

Attacks	UI1	UI3	UI5	UI7
Pepper and salt noise (SPN)	0.001	0.9994	0.9996	0.9997
	0.01	0.9992	0.9995	0.9995
Gaussian attack (GN)	0.001	0.9993	0.9992	0.9994
	0.01	0.9983	0.9987	0.9982
Speckle attack (SN)	0.001	0.9999	0.9998	0.9998
	0.01	0.9998	0.9999	0.9999
Gaussian low pass filter (GLPF)	3x3	0.9993	0.9995	0.9996
	7x7	0.9991	0.9995	0.9994
Average filter (AF)	3x3	0.9990	0.9991	0.9991
	7x7	0.9985	0.9987	0.9989
Median filter (MF)	3x3	0.9994	0.9995	0.9994
	7x7	0.9991	0.9992	0.9988
Rotation (RN)	1	0.9994	0.9996	0.9997
	5	0.9991	0.9990	0.9989
Histogram equalization (HE)		0.9861	0.9874	0.9870
		0.9873		
Sharpening (SH)	4	0.9961	0.9942	0.9951
		0.9953		
JPEG	25	0.9998	0.9997	0.9997
		0.9998		
JPEG 2000	10	0.9999	0.9999	0.9998
		0.9999		
Motion blur (MB)	5, 5	0.9991	0.9994	0.9994
		0.9992		
Shearing (SG)	0.15	0.9994	0.9994	0.9995
		0.9996		
ROI-filter (ROIF)		0.9992	0.9992	0.9994
		0.9993		

Table 3. NCC values against combinational attacks.

Combinational Attacks	UI2	UI4	UI6	UI8
SPN (0.001) + SN (0.001)	0.9889	0.9859	0.9819	0.9836
GN (0.001) + SN (0.001)	0.9817	0.9805	0.9819	0.9825
SPN (0.001) + GN (0.001)	0.9869	0.9870	0.9850	0.9870
AF (3x3) + MF (3x3)	0.9834	0.9653	0.9669	0.9739
Weiner filter (3x3) + MF (3x3)	0.9856	0.9666	0.9657	0.9779
GLPF (3x3) + SPN (0.0001)	0.9847	0.9839	0.9836	0.9839
JPEG (25) + JPEG2000 (10)	0.9857	0.9833	0.9839	0.9864
JPEG (10) + ROI filtering (3x3)	0.9837	0.9786	0.9710	0.9835
RN (2) + JPEG (25)	0.9747	0.9774	0.9737	0.9706

in an image whose area is almost constant throughout a continuous range of intensity thresholds. A continuous group of pixels whose all pixel intensities are either greater (bright extremal regions) or lower (dark extremal regions) than those of its boundary is formally referred to as an extremal area. When the relative change in a region's area with respect to changes in threshold intensity reaches a local minimum, the region is considered maximally stable. This stability requirement makes MSER exceptionally reliable in low-texture or medical imaging contexts by allowing it to identify repetitive and discriminative regions without depending on gradient magnitude or direction [6]. MSER regions are intrinsic, content-dependent features that are

taken straight from the host image and used in authentication systems [13]. The MSER-based vital feature verification process is depicted in Figure 5. The following are the benefits of MSER-based feature authentication in a medical image watermarking system:

- It keeps clinically important anatomical regions from being altered, ensuring the retention of diagnostic accuracy.
- It allows for content-driven, intrinsic integrity verification without the need for external keys or reference data.
- It facilitates precise detection of alterations and

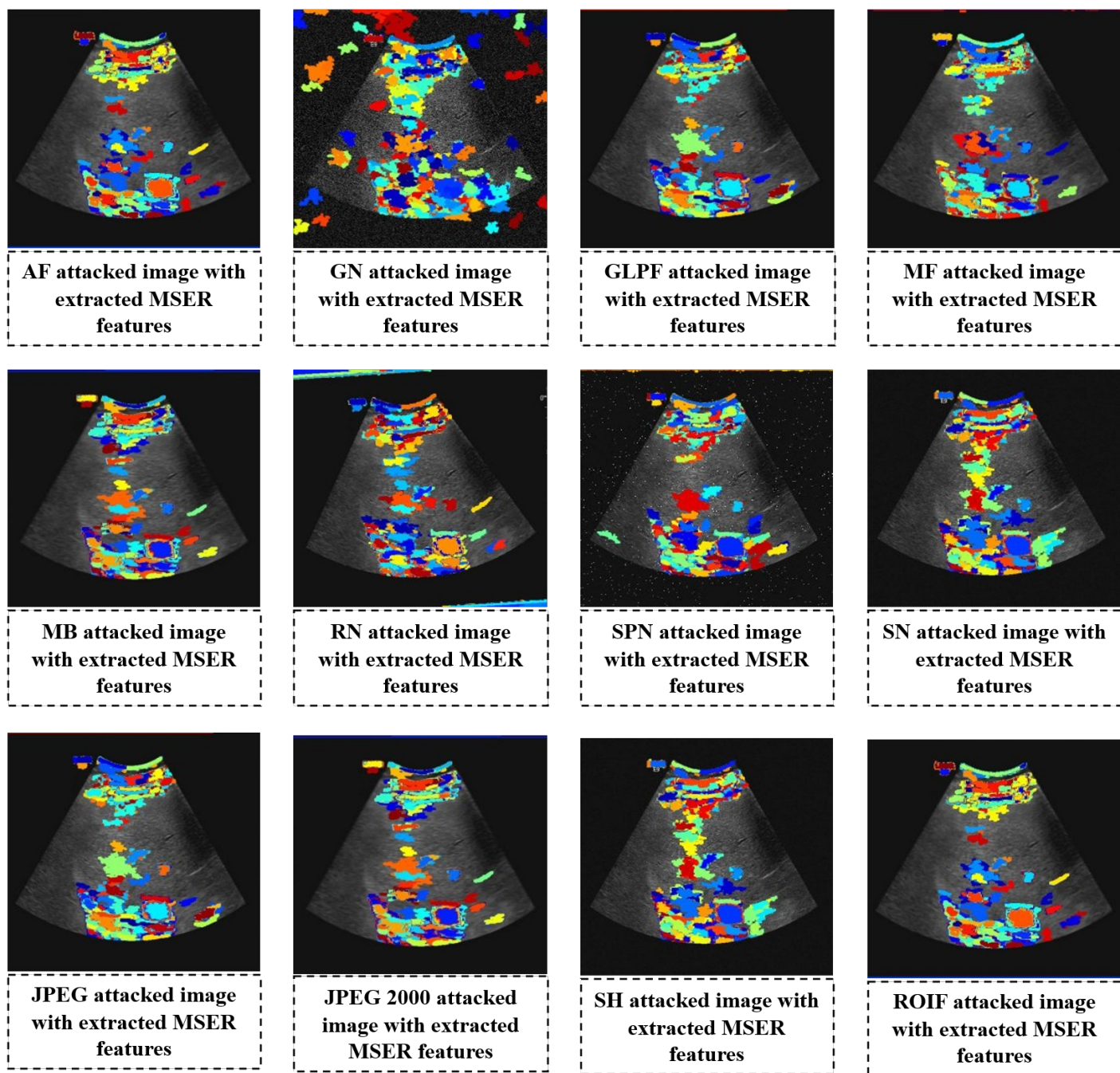


Figure 5. MSER-based vital feature verification.

localization in remote diagnostic procedures and telemedicine.

- It conforms to accepted medical data privacy guidelines and legal frameworks.
- It improves the security and dependability of authentication in ROI-based medical image watermarking systems.
- It maintains authentication reliability while offering resilience against typical image processing operations like compression, filtering,

and noise.

5 Comparative Analysis

In this section, the comparative investigation of the proposed scheme with various existing works is carried out. Table 4 shows the comparison of PSNR and SSIM for robustness. The existing schemes [1–3, 10, 25, 26, 28] have the PSNR values of 38.767 dB, 62.74 dB, 59.91 dB, 51.73 dB, 45.5891 dB, 47.0922 dB, and 45.3362 dB, respectively. On the other hand, the proposed scheme attained the PSNR value of 65.5920 dB, which is higher in comparison with other existing techniques.

The value of the SSIM of the presented work is 1.0000, which is also higher than existing works. This shows the high visual similarity of the presented work in comparison with other methods. Table 5 shows the comparison of NCC values of the proposed work with existing schemes against various attacks for robustness. The presented scheme has much higher NCC values in comparison with [25, 26, 28] against different attacks, which shows the high resilience of the proposed work.

Table 4. Comparison of SSIM and PSNR (Transposed)

	PSNR (dB)	SSIM
[1]	38.767	0.9940
[2]	62.74	0.9998
[3]	59.91	0.9996
[10]	51.73	0.9824
[25]	45.5891	0.9961
[26]	47.0922	0.9918
[28]	45.3362	0.9875
Proposed	65.5920	1.0000

Table 5. Comparison of NCC against attacks.

Attacks	[25]	[26]	[28]	Proposed
SPN (0.001)	0.9981	0.9712	0.9846	0.9997
GN (0.005)	-	0.9856	0.7676	0.9990
SN (0.001)	0.9995	0.9927	0.998	0.9999
GLPF (3x3)	-	0.9915	-	0.9996
RN (1)	-	0.9023	0.9614	0.9997
RN (5)	0.7849	-	-	0.9991
MF (2x2)	0.7549	0.975	0.9759	0.9997
SH	0.8716	0.9905	0.7843	0.9961
HE	0.565	0.8491	0.5007	0.9874
JPEG (10)	0.9391	0.9837	0.9814	0.9998

6 Conclusion

In the proposed work, the vital ROI information of the ultrasound liver image is protected against copyright violations and alterations. The ROI information is detected using a scale-adaptive saliency and statistical information-guided scheme. Then, the integrity of this information is protected by applying the proposed watermarking system using a hybrid fusion of DCT-RDWT-Diag-HD. This scheme enhances the robustness and visual similarity of the input host medical images. SSO is used to get the optimum weighing factor, which further enhances the performance by balancing the properties of the watermarking method. The PSNR value attained

is 65.5920 dB, SSIM is 1.0000 and NCC (without attack) is 1.0000, which shows the effectiveness of the presented work. The presented technique also performs very well against various types of regular and combinational attacks. The presented technique only lacks against geometric and histogram attacks. The results demonstrate that the proposed method is well-suited for protecting the copyright of medical records. In the future, the proposed framework can be extended by applying deep learning methods in ROI detection as well as autoencoders and vision transformer-based watermarking architecture, to secure the integrity of medical records and enhance the performance.

Data Availability Statement

Data will be made available on request.

Funding

This work was supported without any funding.

Conflicts of Interest

The authors declare no conflicts of interest.

AI Use Statement

The authors declare that no generative AI was used in the preparation of this manuscript.

Ethical Approval and Consent to Participate

Not applicable.

References

- [1] Tiwari, A., Awasthi, D., & Srivastava, V. K. (2025). RFPPFMark: robust and false positive problem free image watermarking scheme with its performance comparison by PSO and MRFO in Schur domain. *Signal, Image and Video Processing*, 19(3), 199. [CrossRef]
- [2] Singh, H. K., Baranwal, N., Singh, K. N., & Singh, A. K. (2024). Using multimodal biometric fusion for watermarking of multiple images. *IEEE Transactions on Consumer Electronics*, 70(1), 3487-3494. [CrossRef]
- [3] Singh, H. K., Singh, K. N., & Singh, A. K. (2025). Split ways: Using GAN watermarking for digital image protection with privacy-preserving split model training. *Future Generation Computer Systems*, 163, 107523. [CrossRef]
- [4] Castelli, M., Manzoni, L., Mariot, L., Nobile, M. S., & Tangherloni, A. (2022). Salp swarm optimization: a

critical review. *Expert Systems with Applications*, 189, 116029. [\[CrossRef\]](#)

[5] Abualigah, L., Shehab, M., Alshinwan, M., & Alabool, H. (2020). Salp swarm algorithm: A comprehensive survey. *Neural Computing and Applications*, 32(15), 11195-11215. [\[CrossRef\]](#)

[6] Kimmel, R., Zhang, C., Bronstein, A., & Bronstein, M. (2011). Are MSER features really interesting?. *IEEE Transactions on Pattern Analysis and Machine Intelligence*, 33(11), 2316-2320. [\[CrossRef\]](#)

[7] Eswaraiah, R., & Sreenivasa Reddy, E. (2014). Medical image watermarking technique for accurate tamper detection in ROI and exact recovery of ROI. *International Journal of Telemedicine and Applications*, 2014(1), 984646. [\[CrossRef\]](#)

[8] Ravichandran, D., Praveenkumar, P., Rajagopalan, S., Rayappan, J. B. B., & Amirtharajan, R. (2021). ROI-based medical image watermarking for accurate tamper detection, localisation and recovery. *Medical & Biological Engineering & Computing*, 59(6), 1355-1372. [\[CrossRef\]](#)

[9] Das, S., & Kundu, M. K. (2013). Effective management of medical information through ROI-lossless fragile image watermarking technique. *Computer Methods and Programs in Biomedicine*, 111(3), 662-675. [\[CrossRef\]](#)

[10] Eswaraiah, R., & Sreenivasa Reddy, E. (2015). Robust medical image watermarking technique for accurate detection of tampers inside region of interest and recovering original region of interest. *IET Image Processing*, 9(8), 615-625. [\[CrossRef\]](#)

[11] Keshavarzian, R., & Aghagolzadeh, A. (2016). ROI based robust and secure image watermarking using DWT and Arnold map. *AEU-International Journal of Electronics and Communications*, 70(3), 278-288. [\[CrossRef\]](#)

[12] Bhalerao, S., Ansari, I. A., & Kumar, A. (2023). A reversible medical image watermarking for ROI tamper detection and recovery. *Circuits, Systems, and Signal Processing*, 42(11), 6701-6725. [\[CrossRef\]](#)

[13] Awasthi, D., & Srivastava, V. K. (2025). ROI-based optimized image watermarking with real-time authentication. *Cluster Computing*, 28(7), 463. [\[CrossRef\]](#)

[14] Qasim, A. F., Aspin, R., Meziane, F., & Hogg, P. (2019). ROI-based reversible watermarking scheme for ensuring the integrity and authenticity of DICOM MR images. *Multimedia Tools and Applications*, 78(12), 16433-16463. [\[CrossRef\]](#)

[15] Alshanbari, H. S. (2021). Medical image watermarking for ownership & tamper detection. *Multimedia Tools and Applications*, 80(11), 16549-16564. [\[CrossRef\]](#)

[16] Awasthi, D., Khare, P., Srivastava, V. K., Singh, A. K., & Gupta, B. B. (2025). DeepNet: Protection of deepfake images with aid of deep learning networks. *Image and Vision Computing*, 158, 105540. [\[CrossRef\]](#)

[17] Awasthi, D., Khare, P., & Srivastava, V. K. (2025). ANFISmark: ANFIS-based secure watermarking approach for telemedicine applications. *Neural Computing and Applications*, 37(14), 8677-8698. [\[CrossRef\]](#)

[18] Dwivedi, R., Awasthi, D., & Srivastava, V. K. (2025). WSOMedMark: Robust and optimized dual image watermarking using RDWT and its authentication using BRISK and MSER features for smart healthcare system. *Multimedia Tools and Applications*, 84(14), 13653-13690. [\[CrossRef\]](#)

[19] Singh, H., Deshmukh, M., & Awasthi, L. K. (2025). Secure healthcare data management using multimodal image fusion and dual watermarking. *Scientific Reports*, 15(1), 9047. [\[CrossRef\]](#)

[20] Saïd, B. A., Ali, W., Amine, K., Redouane, K. M., & Sahu, A. K. (2025). Robust medical image watermarking based on Ridgelet transform and Ant Colony Optimization for telemedicine security. *Systems and Soft Computing*, 200390. [\[CrossRef\]](#)

[21] Gupta, A. K., Chakraborty, C., & Gupta, B. (2025). Bio-inspired optimization based secure model for watermarking of medical data. *Multimedia Tools and Applications*, 1-31. [\[CrossRef\]](#)

[22] Zhang, G. D., Zhang, Z. X., Li, J. Y., Guo, Y., Ding, H., Xi, X. T., ... & Han, Y. C. (2025). Robust Image Watermarking in Wavelet Domain using RDWT-HD-SVD and Whale Optimization Algorithm. *Circuits, Systems, and Signal Processing*, 44(4), 2681-2705. [\[CrossRef\]](#)

[23] Tiwari, A., & Srivastava, V. K. (2025). MIWHSmark: Multiple Image Watermarking Based on Hybrid Technique in Schur Domain for Smart Healthcare System. *Circuits, Systems, and Signal Processing*, 1-38. [\[CrossRef\]](#)

[24] Mirjalili, S., Gandomi, A. H., Mirjalili, S. Z., Saremi, S., Faris, H., & Mirjalili, S. M. (2017). Salp swarm algorithm: A bio-inspired optimizer for engineering design problems. *Advances in Engineering Software*, 114, 163-191. [\[CrossRef\]](#)

[25] Anand, A., & Singh, A. K. (2022). Hybrid nature-inspired optimization and encryption-based watermarking for e-healthcare. *IEEE Transactions on Computational Social Systems*, 10(4), 2033-2040. [\[CrossRef\]](#)

[26] Anand, A., & Singh, A. K. (2022). Dual watermarking for security of COVID-19 patient record. *IEEE Transactions on Dependable and Secure Computing*, 20(1), 859-866. [\[CrossRef\]](#)

[27] Clark, K., Vendt, B., Smith, K., Freymann, J., Kirby, J., Koppel, P., ... & Tarbox, L. (2013). The Cancer Imaging Archive (TCIA): Maintaining and operating a public information repository. *Journal of Digital Imaging*, 26(6), 1045-1057. [\[CrossRef\]](#)

[28] Anand, A., Singh, A. K., Lv, Z., & Bhatnagar, G. (2020). Compression-then-encryption-based secure

watermarking technique for smart healthcare system.
IEEE MultiMedia, 27(4), 133-143. [CrossRef]



Divyanshu Awasthi received his B.Tech in ECE from the University of Allahabad, India in 2018, M.Tech in Signal Processing from Motilal Nehru National Institute of Technology Allahabad, India in 2021, PhD from Motilal Nehru National Institute of Technology Allahabad, India in 2024. Presently, he is working as an Assistant Professor in the Department of Electronics and Communication Engineering at GLA University Mathura, India. He is working on projects related to Digital Image Watermarking. His areas of interest are Digital Image Processing, Signal Processing, Data hiding, Cryptography, and Deep learning. (Email: divyanshu.awasthi@gla.ac.in)



Vinay Kumar Srivastava received the BE degree in Electronics and Telecommunication Engineering from Govt Engineering College Rewa, MP, India, in 1989, the M Tech degree in Communication Engineering from IIT BHU, Varanasi, India, in 1991, and a Ph.D. degree in Electrical Engineering from IIT Kanpur, India in 2001. After spending a brief period in Indian Telephone Industries Limited, Naini, Allahabad, as an Assistant Executive Engineer, he joined Motilal Nehru National Institute of Technology (MNNIT) Allahabad, India, as a Lecturer in 1992, where he became an Assistant Professor in 2001, Associate Professor in 2006 and Professor in 2010. He has about thirty years of teaching and research experience. He has supervised several B Tech projects, M Tech Theses, and Ph.D. Theses. His research areas include signal and image processing, digital image watermarking, compression, multimedia security, and data hiding. (Email: vinay@mnnit.ac.in)